

# Fast Radio Bursts as Standard Candles for Cosmology

Han-Yue Guo<sup>\*</sup> and Hao Wei<sup>†</sup>

*School of Physics, Beijing Institute of Technology, Beijing 100081, China*

## ABSTRACT

Recently, fast radio bursts (FRBs) have become a thriving field in astronomy and cosmology. Due to their extragalactic and cosmological origin, they are useful to study the cosmic expansion and the intergalactic medium (IGM). In the literature, the dispersion measure (DM) of FRB has been considered extensively. It could be used as an indirect proxy of the luminosity distance  $d_L$  of FRB. The observed DM contains the contributions from the Milky Way (MW), the MW halo, IGM, and the host galaxy. Unfortunately, IGM and the host galaxy of FRB are poorly known to date, and hence the large uncertainties of  $DM_{\text{IGM}}$  and  $DM_{\text{host}}$  in DM plague the FRB cosmology. Could we avoid DM in studying cosmology? Could we instead consider the luminosity distance  $d_L$  directly in the FRB cosmology? We are interested to find a way out for this problem in the present work. From the lessons of calibrating type Ia supernovae (SNIa) or long gamma-ray bursts (GRBs) as standard candles, we consider a universal subclassification scheme for FRBs, and there are some empirical relations for them. In the present work, we propose to calibrate type Ib FRBs as standard candles by using a tight empirical relation without DM. The calibrated type Ib FRBs at high redshifts can be used like SNIa to constrain the cosmological models. We also test the key factors affecting the calibration and the cosmological constraints. Notice that the results are speculative, since they are based on simulations for the future (instead of now). We stress that the point in the present work is just to propose a viable method and a workable pipeline using type Ib FRBs as standard candles for cosmology in the future.

PACS numbers: 98.80.Es, 98.70.Dk, 98.70.-f, 97.10.Bt, 98.62.Py

---

<sup>\*</sup> email address: guohanyue7@163.com

<sup>†</sup> Corresponding author; email address: haowei@bit.edu.cn

## I. INTRODUCTION

Recently, fast radio bursts (FRBs) have become a thriving field in astronomy and cosmology [1–7]. FRBs are millisecond-duration transient radio sources, and their origin is still unknown to date. Most of them are at extragalactic/cosmological distances, as suggested by their large dispersion measures (DMs) well in excess of the Galactic values. Therefore, it is of interest to study cosmology and the intergalactic medium (IGM) with FRBs [1–7].

To date, there are many FRB theories in the literature [1–7, 62]. For example, FRBs might originate from magnetars, mergers/interactions of compact objects (such as neutron star (NS), white dwarf (WD), black hole (BH), strange star (SS), axion star), collapse of compact objects, active galactic nuclei (AGN), supernovae remnants (SNR), starquakes, giant pulses, superradiance, collision/interaction between NS and asteroids/comets, cosmic strings, cosmic combs, pulsar lightnings, variable stars, wandering pulsar beams. We strongly refer to [62] for the living FRB theory catalogue.

As is well known, one of the key observational quantities of FRBs is the dispersion measure (DM), namely the column density of the free electrons, due to the ionized medium (plasma) along the path. Since the distance along the path in DM records the expansion history of the universe, it plays a key role in the FRB cosmology. The observed DM of FRB at redshift  $z$  can be separated into [8–16]

$$\text{DM}_{\text{obs}} = \text{DM}_{\text{MW}} + \text{DM}_{\text{halo}} + \text{DM}_{\text{IGM}} + \text{DM}_{\text{host}}/(1+z), \quad (1)$$

where  $\text{DM}_{\text{MW}}$ ,  $\text{DM}_{\text{halo}}$ ,  $\text{DM}_{\text{IGM}}$ ,  $\text{DM}_{\text{host}}$  are the contributions from the Milky Way (MW), the MW halo, IGM, the host galaxy (including interstellar medium of the host galaxy and the near-source plasma), respectively. Obviously, the main contribution to DM of FRB comes from IGM. The mean of  $\text{DM}_{\text{IGM}}$  is given by [8–16]

$$\langle \text{DM}_{\text{IGM}} \rangle = \frac{3cH_0\Omega_b}{8\pi Gm_p} \int_0^z \frac{f_{\text{IGM}}(\tilde{z}) f_e(\tilde{z}) (1+\tilde{z}) d\tilde{z}}{h(\tilde{z})}, \quad (2)$$

where  $c$  is the speed of light,  $H_0$  is the Hubble constant,  $\Omega_b$  is the present fractional density of baryons,  $G$  is the gravitational constant,  $m_p$  is the mass of proton,  $h(z) \equiv H(z)/H_0$  is the dimensionless Hubble parameter,  $f_{\text{IGM}}(z)$  is the fraction of baryon mass in IGM, and  $f_e(z)$  is the ionized electron number fraction per baryon. The latter two are functions of redshift  $z$  in principle.

One can see that  $\langle \text{DM}_{\text{IGM}} \rangle$  is related to the expansion history of the universe through  $h(z)$  according to Eq. (2). Note that  $\langle \text{DM}_{\text{IGM}} \rangle$  is the mean value of  $\text{DM}_{\text{IGM}}$  in all directions of the lines of sight. This is only valid due to the well-known cosmological principle, which assumes that the universe is homogeneous and isotropic on cosmic/large scales. However, it is not homogeneous and isotropic on local/small scales. Thus,  $\text{DM}_{\text{IGM}} \neq \langle \text{DM}_{\text{IGM}} \rangle$  for most observed FRB, since the plasma density fluctuates along the line of sight [17–20] (see also e.g. [8–16]). In the literature, the deviation of  $\text{DM}_{\text{IGM}}$  from  $\langle \text{DM}_{\text{IGM}} \rangle$  is usually characterized by the uncertainty  $\sigma_{\text{IGM}}(z)$ , which is a function of redshift  $z$  in principle. Unfortunately, IGM is poorly known in fact. So, one can only consider various empirical  $\sigma_{\text{IGM}}(z)$  in the literature, which is usually large ( $\sim \mathcal{O}(10^2)$  to  $\mathcal{O}(10^3)$  pc cm<sup>-3</sup>) [17–20] (see also e.g. [8–16]). In fact, the large uncertainty  $\sigma_{\text{IGM}}(z)$  in  $\text{DM}_{\text{IGM}}$  is one of the main troubles in the FRB cosmology. On the other hand,  $f_{\text{IGM}}(z)$  and  $f_e(z)$  in  $\langle \text{DM}_{\text{IGM}} \rangle$  are both functions of redshift  $z$  in principle. Since we are rather ignorant of IGM and the cosmic ionization history,  $f_{\text{IGM}}$  and  $f_e$  have been extensively assumed to be constant in the literature. Thus, this also leads to uncertainties in the FRB cosmology.

For convenience, one can introduce the extragalactic DM [8–16], namely

$$\text{DM}_{\text{E}} = \text{DM}_{\text{obs}} - \text{DM}_{\text{MW}} - \text{DM}_{\text{halo}} = \text{DM}_{\text{IGM}} + \text{DM}_{\text{host}}/(1+z). \quad (3)$$

In the literature,  $\text{DM}_{\text{E}}$  has been extensively used to study cosmology. Note that the host galaxy of FRB and hence its contribution to DM are also poorly known. So,  $\text{DM}_{\text{host}}$  was usually assumed to be constant or was randomly assigned from some simplified distributions in the literature [8–16]. Of course, these simplifications prevent us from better understanding the cosmic expansion history. Here we refer to e.g. the highly cited Ref. [20] for a qualitative impression on the cosmological constraints. In [20], using  $\text{DM}_{\text{E}}$  of 100 simulated FRBs to constrain the flat  $\Lambda$ CDM model,  $\Omega_m = 0.29 \pm 0.10$  and  $0.26 \pm 0.05$  were found for the cases of  $z_{\text{max}} = 1.5$  and 2.5, respectively. To improve the cosmological constraints, it is common to

combine FRBs with other observations such as type Ia supernovae (SNIa), cosmic microwave background (CMB), and baryon acoustic oscillations (BAO) in the literature. However, such improvements are mainly dominated by SNIa, CMB and BAO, rather than FRBs themselves.

Although DM is extensively used to study cosmology in the literature, it is just an indirect proxy of the luminosity distance  $d_L$  of FRB. In addition, the large uncertainties of  $DM_{\text{IGM}}$  and  $DM_{\text{host}}$  in DM plague the FRB cosmology, as mentioned above. Could we avoid DM in studying cosmology? Could we instead consider the luminosity distance  $d_L$  directly in the FRB cosmology? We are interested to find a way out for this problem in the present work.

Of course, it is difficult to obtain the luminosity distance  $d_L$  of FRB. If this FRB is well localized to a host galaxy, and the luminosity distance of this galaxy has been well measured,  $d_L$  of this FRB is equal to the one of its host galaxy. Alternatively, if the luminosity distance of objects in the same host galaxy of an FRB (e.g. supernova, gamma-ray burst, or gravitational wave event, not necessarily counterparts) can be measured,  $d_L$  of this FRB is also on hand. But these make sense only at low redshifts. We should find a new method to obtain the luminosity distances  $d_L$  for FRBs at high redshifts.

History always repeats itself. As is well known, the distance ladder has been used in many neighboring fields. For example, the luminosity distances of Cepheids can be obtained by using the empirical period versus luminosity ( $P - L$ , or, Leavitt) relation [21]. If a type Ia supernova (SNIa) shares the same host galaxy with a Cepheid, the luminosity distance of this SNIa is equal to the one of Cepheid. The empirical SNIa light-curve versus luminosity (Phillips) relation [22] could be calibrated by using these SNIa at low redshifts. Thus, the luminosity distances of SNIa at high redshifts can be obtained by extending the calibrated SNIa Phillips relation [23]. Similar to the case of calibrating SNIa as secondary standard candles by using Cepheids as primary standard candles, this has also been considered in the field of gamma-ray bursts (GRBs). The luminosity distances of long GRBs at low redshifts can be obtained by using e.g. interpolation from the ones of SNIa at nearby redshifts [24, 25]. Various empirical relations, especially the  $E_{\text{p},i} - E_{\text{iso}}$  (Amati) relation [26], could be calibrated by using these long GRBs at low redshifts [27] (see also e.g. [24, 25]). Thus, the luminosity distances of long GRBs at high redshifts can be obtained by extending the calibrated GRB empirical relation(s) [24, 25, 28, 29].

The lessons from the above history of calibrating SNIa or long GRBs as standard candles are (a) at least a tight empirical relation involving the luminosity distance is necessary; (b) the empirical relations are only valid for some subclasses, namely SNIa (not for type Ib, Ic and II supernovae), or long GRBs (not for short GRBs). In the present work, we try to calibrate FRBs as standard candles. Thus, we should introduce a universal subclassification scheme for FRBs, and find a tight empirical relation involving the luminosity distance for a subclass of FRBs. Fortunately, they are ready in our previous works.

This paper is organized as followings. In Sec. II, we briefly introduce the universal subclassification scheme and the empirical relations for FRBs. In Sec. III, we describe the method to calibrate type Ib FRBs as standard candles. In Sec. IV, we test the key factors affecting the calibration and the cosmological constraints. In Sec. V, some brief concluding remarks are given.

## II. SUBCLASSIFICATION AND EMPIRICAL RELATIONS FOR FRBS

One of the interesting topics is the classification of FRBs, which is closely related to the origin of FRBs. Clearly, different physical mechanisms are required by different classes of FRBs. Well motivated by the actual observations, they are usually classified into two populations: non-repeating FRBs and repeating FRBs [1–7]. For convenience, we call them type I and II FRBs in [16], respectively.

In the literature, it was speculated for a long time that the FRB distribution tracks the cosmic star formation history (SFH) [1–7]. The well-known Galactic FRB 200428 associated with the young magnetar SGR 1935+2154 [30–33] confirmed that some FRBs originate from young magnetars. On the other hand, some repeating FRBs (such as FRB 121102, FRB 180916.J0158+65, FRB 20190520B, FRB 20181030A) were observed to be closely correlated with star-forming activities [34–37]. Therefore, it is reasonable to expect that at least some (if not all) FRBs are associated with young stellar populations, and hence their distribution tracks SFH. However, this speculation was challenged recently. The well-known repeating FRB 20200120E in a globular cluster of the nearby galaxy M81 [38–40] suggested that some FRBs are associated with old stellar populations instead. In addition, the host of non-repeating FRB 20210117A was also found to be a dwarf galaxy with little on-going star formation [57]. The host of FRB 20220509G

|                                  |   |   |
|----------------------------------|---|---|
| <b>FRBs</b>                      | <b>Class (a) :</b><br>associated with old stellar populations                     | <b>Class (b) :</b><br>associated with young stellar populations                     |
| <b>Type I :</b><br>Non-repeating | <b>Type Ia :</b><br>Non-repeating FRBs<br>associated with old stellar populations | <b>Type Ib :</b><br>Non-repeating FRBs<br>associated with young stellar populations |
| <b>Type II :</b><br>Repeating    | <b>Type IIa :</b><br>Repeating FRBs<br>associated with old stellar populations    | <b>Type IIb :</b><br>Repeating FRBs<br>associated with young stellar populations    |

TABLE I: A universal subclassification scheme for FRBs proposed in [16].

is a red, old, massive elliptical galaxy with low star formation rate [58]. We refer to e.g. [59, 60] for more examples requiring FRB progenitor formation channels associated with old stellar populations. On the other hand, it was claimed in [41] that the 536 bursts of the first CHIME/FRB catalog [42] (released in June 2021, including 474 one-off bursts and 62 repeat bursts from 18 repeaters observed at the central frequency  $\nu_c = 600$  MHz) as a whole do not track SFH. In [15], it was independently confirmed that the FRB distribution tracking SFH can be rejected at high confidence, and a suppressed evolution (delay) with respect to SFH was found.

The above discussions based on the actual observations have motivated us in [16] to speculate that some FRBs are associated with young populations and hence their distribution tracks SFH, while the other FRBs are associated with old populations and hence their distribution does not track SFH. This led us to propose a universal subclassification scheme for FRBs [16], as shown in Table I.

In [16], we have conducted this subclassification scheme for FRBs by using the actual data of the first CHIME/FRB catalog [42]. These FRBs are subclassified in the transient duration  $\nu W$  versus spectral luminosity  $L_\nu$  phase plane, with some isothermal lines of brightness temperature  $T_B$ . The  $\nu W - L_\nu$  phase plane has been divided into ten regions by three dividing lines  $\nu W = 10^{-3}$  GHz s,  $L_\nu = 10^{34}$  erg/s/Hz and  $T_B = 2 \times 10^{35}$  K, which are determined by the minimal p-values of Kolmogorov-Smirnov (KS) test [16]. Note that there are 430 non-repeating (type I) FRBs after the robust cut in the first CHIME/FRB catalog [42]. Then, we test these 10 regions one by one. For each region, 430 type I FRBs are divided into two samples inside or outside this region. We compare their redshift distributions by using KS test, and also check whether one of these two sample tracks SFH by using the method proposed in [15, 41, 43]. Finally, we find that region (8) is very successful, and hence the physical criteria for the subclassification of type I FRBs have been clearly determined [16], namely

$$\text{Type Ia : } L_\nu \leq 10^{34} \text{ erg/s/Hz} \quad \& \quad T_B \geq 2 \times 10^{35} \text{ K}, \quad (4)$$

$$\text{Type Ib : } \text{otherwise}. \quad (5)$$

Note that these physical criteria are suitable for the first CHIME/FRB catalog [42], and they might be changed for the larger and better FRB datasets in the future, but the universal subclassification scheme given in Table I will always hold. We find that in the first CHIME/FRB catalog [42], 65 type Ia FRBs do not track SFH, but 365 type Ib FRBs do track SFH at high confidence. Similarly, we speculate that the possible physical criteria for the subclassification of type II FRBs might be given by [16]

$$\text{Type IIa : } L_\nu \lesssim 10^{29} \text{ erg/s/Hz} \quad \& \quad T_B \gtrsim 10^{30} \text{ K}, \quad (6)$$

$$\text{Type IIb : } \text{otherwise}. \quad (7)$$

We stress that they are highly speculative, because there are only 17 repeaters after the robust cut in the first CHIME/FRB catalog [42], which are too few to form a good enough sample in statistics. Since the data of repeaters will be rapidly accumulated in the future, we hope this subclassification of type II FRBs could be refined. We strongly refer to [16] for the technical details of the subclassification.

As mentioned in [16], there might be three methods to identify type Ib FRBs: (a) Their distribution tracks SFH. But this does not work for an individual FRB. (b) The physical criteria similar to Eqs. (4)

and (5). But this heavily depends on cosmology, and a circularity problem might exist. (c) The precise localizations of FRBs. We strongly prefer the last method (c) in practice. If a non-repeating (type I) FRB has been precisely localized by using e.g. VLBI down to the milliarcsecond level [44, 45] or better in the future, its host galaxy and local environment could be well determined. Subsequently, it is a type Ib FRB if this FRB lives in a star-forming environment. Of course, its redshift can also be identified accordingly in this way. We stress that no circularity problem exists in fact by using the method (c). To date, a few dozens of non-repeating FRBs associated with young stellar populations (namely type Ib FRBs) have been already determined by the method (c) using telescopes/arrays such as DSA-110, ASKAP, Arecibo, Parkes, FAST and EVN, as summarized in Table II of [61]. Actually, the method (c) “precise localizations of FRBs” is the main way to determine type Ib FRBs without circularity problem in practice.

In [16], we have found that there are some tight empirical relations for type Ia FRBs but not for type Ib FRBs, and vice versa. These make them different in physical properties. Notice that there are only 17 repeaters after the robust cut in the first CHIME/FRB catalog [42], no empirical relations found for type II FRBs in [16]. On the other hand, there are 65/365 type Ia/Ib FRBs after the robust cut in the first CHIME/FRB catalog [42], respectively. Type Ib FRBs dominate obviously, and hence the empirical relations for them are much tighter than the ones for type Ia FRBs. Unfortunately, the empirical relations only for type Ia FRBs found in [16] do not involve the luminosity distance. In addition, type Ib FRBs are associated with young stellar populations, and hence their distribution tracks SFH. This remarkably facilitates generating the mock type Ib FRBs in simulations. Thus, we choose to only calibrate type Ib FRBs as standard candles in the present work.

Actually, we found some tight empirical relations between spectral luminosity  $L_\nu$ , isotropic energy  $E$  and  $\text{DM}_E$  for type Ib FRBs in [16], where  $\text{DM}_E$  is given by Eq. (3), and

$$L_\nu = 4\pi d_L^2 S_\nu, \quad E = 4\pi d_L^2 \nu_c F_\nu / (1+z), \quad (8)$$

in which  $d_L$  is the luminosity distance,  $S_\nu$  is the flux,  $F_\nu$  is the specific fluence,  $\nu_c$  is the central observing frequency ( $\nu_c = 600$  MHz for CHIME [42]). The 2-D empirical relations for 365 type Ib FRBs in the first CHIME/FRB catalog are given by [16]

$$\log E = 0.8862 \log L_\nu + 10.0664, \quad (9)$$

$$\log L_\nu = 2.4707 \log \text{DM}_E + 27.3976, \quad (10)$$

$$\log E = 2.2345 \log \text{DM}_E + 34.2238, \quad (11)$$

where “log” gives the logarithm to base 10, and  $E$ ,  $L_\nu$ ,  $\text{DM}_E$  are in units of erg, erg/s/Hz,  $\text{pc cm}^{-3}$ , respectively. In the light of the 2-D empirical relations given by Eqs. (9)–(11), it is anticipated that there is a tight 3-D empirical relation between spectral luminosity  $L_\nu$ , isotropic energy  $E$  and  $\text{DM}_E$ . Fitting to the data, we also found this 3-D empirical relation in [16] for 365 type Ib FRBs in the first CHIME/FRB catalog, namely

$$\log L_\nu = 1.1330 \log \text{DM}_E + 0.5986 \log E + 6.9098. \quad (12)$$

Noting that the empirical relations in Eqs. (10)–(12) involve  $\text{DM}_E$ , they are not suitable for our goal, as mentioned in Sec. I. Fortunately, the empirical relation in Eq. (9) does not involve DM, but it does involve the luminosity distance  $d_L$  (n.b. Eq. (8)), and hence it works well for calibrating type Ib FRBs as standard candles. We strongly refer to [16] for the technical details of the empirical relations.

Further, these empirical relations have been checked in [61] with the current 44  $\sim$  52 localized FRBs (most of them are type Ib FRBs). In [16], the errors were not taken into account. But we have considered the errors by using the actual data (rather than simulations) in Sec. IV of [61], and found that

$$\log E = a \log L_\nu + b \quad \text{with} \quad a = 0.8336 \pm 0.0375, \quad b = 11.7858 \pm 1.2568, \quad \sigma_{\text{int}} = 0.3308, \quad (13)$$

$$\log L_\nu = a \log \text{DM}_E + b \quad \text{with} \quad a = 2.3741 \pm 0.4527, \quad b = 27.8054 \pm 1.0893, \quad \sigma_{\text{int}} = 1.2292, \quad (14)$$

$$\log E = a \log \text{DM}_E + b \quad \text{with} \quad a = 2.1807 \pm 0.3967, \quad b = 34.4443 \pm 0.9568, \quad \sigma_{\text{int}} = 1.0591, \quad (15)$$

where the constraints on slope  $a$  and intercept  $b$  are given by their means with  $1\sigma$  uncertainties. The  $1\sigma$ ,  $2\sigma$  and  $3\sigma$  contours for  $a$  and  $b$  of these empirical relations have also been given in Sec. IV of [61]. It is reasonable to expect that the errors will be significantly decreased in the future with a large amount of well-localized type Ib FRBs.

### III. CALIBRATING TYPE IB FRBS AS STANDARD CANDLES

It is worth noting that the above empirical relations were found by using the first CHIME/FRB catalog [42], and the values of slopes and intercepts might be changed for the larger and better FRB datasets in the future. So, one should not persist in their (exact) numerical values. The key point is that these empirical relations do exist in such forms for type Ib FRBs.

Here, we assume that the empirical  $L_\nu - E$  relation really exists due to the unknown physical mechanism for the origins of type Ib FRBs. It takes the form of Eq. (9), namely

$$\log \frac{E}{\text{erg}} = a \log \frac{L_\nu}{\text{erg/s/Hz}} + b, \quad (16)$$

where  $a$  and  $b$  are both dimensionless constants. In particular,  $a = 0.8862$  and  $b = 10.0664$  [16] for 365 type Ib FRBs in the first CHIME/FRB catalog. Note that the luminosity distance  $d_L$  is implicit in the empirical  $L_\nu - E$  relation given by Eq. (16). Using Eq. (8), we recast Eq. (16) as

$$\mu = -\frac{5}{2(1-\alpha)} \log \frac{F_\nu/(1+z)}{\text{Jy ms}} + \frac{5\alpha}{2(1-\alpha)} \log \frac{S_\nu}{\text{Jy}} + \beta, \quad (17)$$

where  $\alpha = a \neq 1$ ,  $\beta = \text{const.}$  is a complicated combination of  $a$ ,  $b$ ,  $\nu_c/\text{MHz}$ , and  $\mu$  is the well-known distance modulus defined by

$$\mu = 5 \log \frac{d_L}{\text{Mpc}} + 25. \quad (18)$$

Unlike  $L_\nu$  and  $E$  in Eq. (16), we note that  $F_\nu$ ,  $S_\nu$  and  $\mu$  (equivalently  $d_L$ ) are all observed quantities, and hence it is more convenient to instead use Eq. (17) in calibrating type Ib FRBs as standard candles. There are two free parameters  $\alpha$  and  $\beta$  in Eq. (17), and they will be calibrated by using type Ib FRBs at low redshifts.

Of course, current data of FRBs are certainly not enough to calibrate type Ib FRBs as standard candles. So, it will be a proof of concept by using the simulated FRBs in the present work. We assume that there will be a large amount of type Ib FRBs with identified redshifts in the future. If a non-repeating (type I) FRB has been precisely localized by using e.g. VLBI down to the milliarcsecond level [44, 45] or better in the future, its host galaxy and local environment can be well determined. Subsequently, it is a type Ib FRB if this FRB lives in a star-forming environment. Its redshift could be identified by using the spectra of the host galaxy. Actually, as summarized in Table II of [61], 52 localized FRBs (most of them are type Ib FRBs) were found recently by using telescopes/arrays such as DSA-110, ASKAP, Arecibo, Parkes, FAST and EVN. After Ref. [61] has been submitted to arXiv, another 48 new localized FRBs (most of them are type Ib FRBs) were released in e.g. [63–65]. Note that almost all these  $\sim 100$  localized FRBs (most of them are type Ib FRBs) were observed and localized in the recent  $2 \sim 3$  years. Actually, many new and powerful projects to precisely localize FRBs have been proposed and under construction, such as DSA-2000, FASTA, CHIME/FRB outriggers and EVN. Therefore, it is reasonable to expect that in the near future ( $3 \sim 5$  years) there will be a large amount ( $300 \sim 500$ ) of type Ib FRBs with identified redshifts, and the number might be  $\sim \mathcal{O}(10^3)$  in the next 10 years.

On the other hand, the luminosity distance  $d_L$  (equivalently the distance modulus  $\mu$ ) of type Ib FRBs should be independently measured to build the Hubble diagram. This is a fairly difficult task at high redshifts. But it is possible to measure the luminosity distance of type Ib FRBs at enough low redshifts. Fortunately, the redshift range of FRBs is very wide. They could be at very high redshifts  $z > 3$  (even  $z \sim 15$  [46]), and hence they might be a powerful probe for the early universe. On the other hand, they can also be at very low redshifts, even in our Milky Way ( $z = 0$ ) as shown by the Galactic FRB 200428. In fact, many nearby FRBs at very low identified redshifts were found [47]. Thus, it is possible that a type Ib FRB and a SNIa or a Cepheid are in the same host galaxy, and hence the luminosity distance  $d_L$  (equivalently the distance modulus  $\mu$ ) of type Ib FRB is equal to the one of SNIa or Cepheid. Note that type Ib FRB and SNIa/Cepheid are not necessarily associated. This is just similar to the case of calibrating SNIa as standard candles by using Cepheids, as mentioned in Sec. I. Because Cepheids are certainly at very low redshifts and SNIa can be at not so low redshifts (for example,  $z \sim 0.1$  or  $0.5$ ), we

only consider the case of SNIa in this work. As is well known, currently the distance modulus  $\mu$  of SNIa can be measured very precisely. It is also expected that the precision will be significantly improved in the future. Thus, it is reasonable to assume that the distance modulus  $\mu$  of type Ib FRB at low redshifts could also be measured in the future with the precision comparable with the one of SNIa.

If the number of type Ib FRBs at low redshifts with measured distance moduli  $\mu$ , redshifts  $z$ , fluence  $F_\nu$  and flux  $S_\nu$  is large enough, the empirical relation in Eq. (17) could be well calibrated by fitting it to these type Ib FRBs (note that “how many type Ib FRBs are large enough” is the object to be studied in Secs. IV B and IV C, and we will soon find that  $N_{\text{FRB}} = 300$  or  $500$  are acceptable, as claimed at the end of Sec. IV C). In this way, the free parameters  $\alpha$  and  $\beta$  in Eq. (17) and their uncertainties will be determined. Then, we assume this calibrated empirical relation in Eq. (17) is universal, namely it also holds at high redshifts (note that the well-known empirical Phillips relation for SNIa [22, 23] and the well-known empirical Amati relation for GRBs [24–29]) are also assumed to be universal due to the (unknown) physical mechanisms (in the case of GRBs it is still unknown to date), but their successful applications in cosmology justified these assumptions. Similarly, it is better to keep an open mind to the universality of the empirical relation for FRBs. In principle, one might test this empirical relation in different redshift ranges and see whether its parameters are consistent (we thank the referee for pointing out this issue), like in the cases of SNIa and GRBs. But currently there are not enough actual data to do this, and we hope it could be done in the next 5 years). Now, for each type Ib FRB at high redshift, its redshift  $z$ , fluence  $F_\nu$  and flux  $S_\nu$  have been observed, and the parameters  $\alpha$ ,  $\beta$  take the same values determined at low redshift in the previous step. Consequently, its distance modulus  $\mu$  (equivalently the luminosity distance  $d_L$ ) in the left hand side of Eq. (17) can be derived since the quantities in the right hand side of Eq. (17) are all known now. Its error  $\sigma_\mu$  can also be obtained by using the error propagation. So, the Hubble diagram of type Ib FRBs at high redshifts is on hand. We can use these type Ib FRBs with known distance moduli  $\mu$ , errors  $\sigma_\mu$ , and redshifts  $z$  to constrain the cosmological models, similar to the case of SNIa.

#### IV. KEY FACTORS AFFECTING THE CALIBRATION AND THE COSMOLOGICAL CONSTRAINTS

As mentioned above, current data of FRBs are not enough to calibrate type Ib FRBs as standard candles. Thus, we have to use the mock type Ib FRBs instead. But the same pipeline holds for the actual type Ib FRBs in the future. In the followings, we briefly describe how to generate the mock type Ib FRBs, and calibrate type Ib FRBs as standard candles. Then, we use the calibrated type Ib FRBs at high redshifts to constrain the cosmological model. Clearly, there are many key factors affecting the calibration and the cosmological constraints. We will test them one by one.

##### A. Generating the mock type Ib FRBs

Here, we generate the mock type Ib FRBs closely following the method used in [15, 16] (see also [41]), but the distribution of type Ib FRBs should track SFH. The mock observed type Ib FRB redshift rate distribution is given by [15, 16, 41]

$$\frac{dN}{dt_{\text{obs}} dz} = \frac{1}{1+z} \cdot \frac{dN}{dt dV} \cdot \frac{c}{H_0} \cdot \frac{4\pi d_C^2}{h(z)}, \quad (19)$$

where the comoving distance  $d_C = d_L/(1+z)$ , and  $dt/dt_{\text{obs}} = (1+z)^{-1}$  due to the cosmic expansion is used. In the present work, we consider the flat  $\Lambda$ CDM cosmology, and hence the dimensionless Hubble parameter  $h(z)$  and the luminosity distance  $d_L$  read

$$h(z) \equiv H(z)/H_0 = \left[ \Omega_m (1+z)^3 + (1-\Omega_m) \right]^{1/2}, \quad d_L = (1+z) \frac{c}{H_0} \int_0^z \frac{d\tilde{z}}{h(\tilde{z})}. \quad (20)$$

Here, we adopt  $\Omega_m = 0.3153$  and  $H_0 = 67.36$  km/s/Mpc from the Planck 2018 results [48]. Since the intrinsic type Ib FRB redshift distribution tracks SFH, we have  $dN/(dt dV) \propto \text{SFH}(z)$ , while the latest

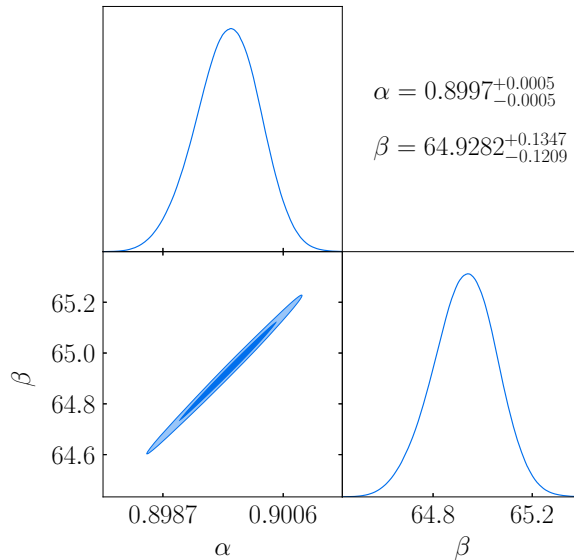


FIG. 1: The marginalized  $1\sigma$  constraints on the parameters  $\alpha$ ,  $\beta$  in the empirical relation (17) and their contours from the data of type Ib FRBs at low redshifts  $z < z_d$  for the fiducial case. Note that in order to better quantify the uncertainties on the parameters  $\alpha$  and  $\beta$ , the fit would need to be performed again after centering the data. See Sec. IV B for details.

result from the observations for SFH is given by [49] (see also [15, 16])

$$\text{SFH}(z) \propto \frac{(1+z)^{2.6}}{1 + ((1+z)/3.2)^{6.2}}. \quad (21)$$

On the other hand, we generate the isotropic energy  $E$  for the mock type Ib FRBs with [15, 16, 41]

$$dN/dE \propto (E/E_c)^{-s} \exp(-E/E_c), \quad (22)$$

where we adopt  $s = 1.9$  and  $\log(E_c/\text{erg}) = 41$ , well consistent with the observations [15, 16]. We generate  $N_{\text{sim}}$  mock type Ib FRBs as follows: (i) for each mock type Ib FRB, randomly assign a mock redshift  $z$  to this FRB from the redshift distribution in Eq. (19); (ii) generate a mock energy  $E_{\text{int}}$  randomly from the distribution in Eq. (22) for this FRB; (iii) derive the luminosity distance  $d_{L,\text{int}}$  and the distance modulus  $\mu_{\text{int}}$  by using Eqs. (20) and (18) with the mock redshift  $z$  for this FRB; (iv) derive the fluence  $F_{\nu,\text{int}}$  by using Eq. (8) with  $E_{\text{int}}$ ,  $d_{L,\text{int}}$ ,  $\nu_c = 600$  MHz (the one of CHIME [42]) and the mock redshift  $z$  for this FRB; (v) assign an error  $\sigma_{F,\text{obs}} = \sigma_{F,\text{rel}} F_{\nu,\text{int}}$  to the “observed” fluence  $F_{\nu,\text{obs}}$  for this FRB, while  $F_{\nu,\text{obs}}$  is randomly assigned from a Gaussian distribution with the mean  $F_{\nu,\text{int}}$  and the standard deviation  $\sigma_{F,\text{obs}}$ . Note that the relative error  $\sigma_{F,\text{rel}}$  will be specified below; (vi) repeat the above steps for  $N_{\text{sim}}$  times. Finally,  $N_{\text{sim}}$  mock type Ib FRBs are on hand.

But these  $N_{\text{sim}}$  mock type Ib FRBs intrinsically generated above are not the ones “detected” by the telescope, due to the telescope’s sensitivity threshold and instrumental selection effects near the threshold. So, the next step is to filter them by using the telescope’s sensitivity model, which is chosen to be the one for CHIME considered in [15, 16, 41]. The sensitivity threshold is  $\log F_{\nu,\text{min}} = -0.5$  for CHIME, where the specific fluence is in units of Jy ms. The FRBs with fluences below this threshold cannot be detected. On the other hand, there is a “gray zone” in the  $\log F_{\nu}$  distribution, within which CHIME has not reached full sensitivity to all sources, due to the direction-dependent sensitivity of the telescope [15, 16, 41]. The detection efficiency parameter in the “gray zone” is given by  $\eta_{\text{det}} = \mathcal{R}^3$ , where  $\mathcal{R} = (\log F_{\nu,\text{th}} - \log F_{\nu,\text{th}}^{\text{min}}) / (\log F_{\nu,\text{th}}^{\text{max}} - \log F_{\nu,\text{th}}^{\text{min}})$ , such that  $\eta_{\text{det}} \rightarrow 0$  at  $\log F_{\nu,\text{th}} = -0.5$  and  $\eta_{\text{det}} \rightarrow 1$  at  $\log F_{\nu,\text{th}}^{\text{max}}$ . Outside the “gray zone”,  $\eta_{\text{det}} = 1$ . For type Ib FRBs tracking SFH, we set  $\log F_{\nu,\text{th}}^{\text{max}} = 0.9$ , which is very close to the best value found in Table II of [16].

In the present work, we generate a pool of mock type Ib FRBs “detected” by the telescope to save the computational power and time. That is, we randomly generate  $N_{\text{sim}} = 500,000,000$  mock type Ib FRBs, and then filter them by using the telescope’s sensitivity model, as mentioned above. Finally, about



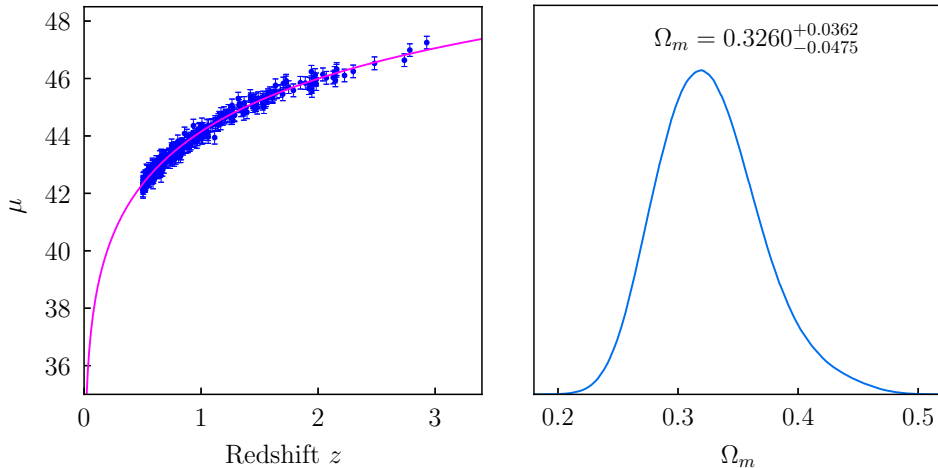


FIG. 2: Left panel: The Hubble diagram  $\mu$  versus  $z$  for type Ib FRBs at high redshifts  $z \geq z_d$ . The magenta line indicates the flat  $\Lambda$ CDM cosmology with the best-fit  $\Omega_m$  given in the right panel. Right panel: The marginalized  $1\sigma$  constraint on the parameter  $\Omega_m$  in the flat  $\Lambda$ CDM cosmology from the data of type Ib FRBs at high redshifts  $z \geq z_d$ . Note that they are both for the fiducial case. See Sec. IV B for details.

40,000 mock “detected” type Ib FRBs after the filter enter this pool. When  $N_{\text{FRB}}$  mock type Ib FRBs are needed in the following subsections, we randomly sample them from this pool.

The next step is to assign the mock flux and its error for each mock type Ib FRB in this pool. We assume that the underlying empirical relation in Eq. (17) is actually

$$\mu = -25 \log \frac{F_\nu / (1+z)}{\text{Jy ms}} + 22.5 \log \frac{S_\nu}{\text{Jy}} + 65, \quad (23)$$

which corresponds to  $\alpha = 0.9$  and  $\beta = 65$ , or equivalently  $a = 0.9$  and  $b \simeq 10.1$  approximately in Eq. (16). We can derive  $S_{\nu, \text{int}}$  by using Eq. (23) with  $\mu_{\text{int}}$ ,  $F_{\nu, \text{int}}$  and the mock redshift  $z$  for this FRB. We assign an error  $\sigma_{S, \text{obs}} = \sigma_{S, \text{rel}} S_{\nu, \text{int}}$  to the “observed” flux  $S_{\nu, \text{obs}}$  for this FRB, while  $S_{\nu, \text{obs}}$  is randomly assigned from a Gaussian distribution with the mean  $S_{\nu, \text{int}}$  and the standard deviation  $\sigma_{S, \text{obs}}$ . Similarly, we assign an error  $\sigma_{\mu, \text{obs}} = \sigma_{\mu, \text{rel}} \mu_{\text{int}}$  to the “observed” distance modulus  $\mu_{\text{obs}}$  for this FRB, while  $\mu_{\text{obs}}$  is randomly assigned from a Gaussian distribution with the mean  $\mu_{\text{int}}$  and the standard deviation  $\sigma_{\mu, \text{obs}}$ . Note that the relative errors  $\sigma_{S, \text{rel}}$  and  $\sigma_{\mu, \text{rel}}$  will be specified below.

So far, a pool of about 40,000 mock “detected” type Ib FRBs with the “observed” redshifts  $z$ , fluences  $F_{\nu, \text{obs}}$  and their errors  $\sigma_{F, \text{obs}}$ , fluxes  $S_{\nu, \text{obs}}$  and their errors  $\sigma_{S, \text{obs}}$ , are ready. In addition, the “observed” distance moduli  $\mu_{\text{obs}}$  and their errors  $\sigma_{\mu, \text{obs}}$  for the mock type Ib FRBs at low redshifts are also on hand. We will pretend to use them as the actual ones blindly in the followings.

## B. The fiducial case

At first, we consider the fiducial case, and the other cases below will be compared with it. In this fiducial case, we consider  $N_{\text{FRB}} = 500$  mock type Ib FRBs, which can be randomly sampled from the pool built in Sec. IV A (note that in principle we could alternatively generate 500 mock type Ib FRBs one by one following the instructions in Sec. IV A, but there is no difference between this way and randomly sampling from the pool. Actually, the mock  $F_\nu$  and  $S_\nu$  are not directly generated. They come from the mock  $d_{L, \text{int}}$  and  $E_{\text{int}}$  (which is randomly sampled from the distribution in Eq. (22) with unequal chance), and they have been filtered by using the telescope’s sensitivity model (namely FRBs are not detected with the same chance), as described in Sec. IV A. Actually, this is a standard pipeline extensively used in the literature). On the other hand, although the fluence and flux of FRBs cannot be measured with high precision currently by the telescope (e.g. CHIME), we assume that they could be measured precisely in the future. So, in the fiducial case, we set the relative errors  $\sigma_{F, \text{rel}}$  and  $\sigma_{S, \text{rel}}$  to be both 1% (frankly, we cannot give the timetable to achieve this goal. But many new and giant telescopes are proposed or under

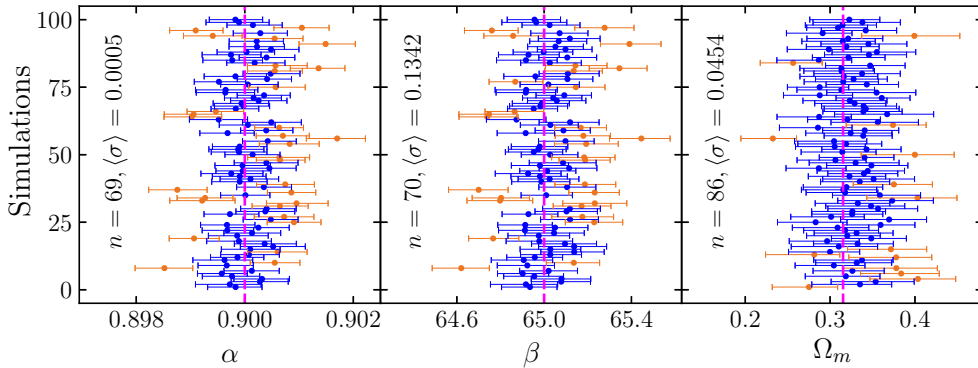


FIG. 3: The marginalized  $1\sigma$  constraints on the parameters  $\alpha$  (left panel),  $\beta$  (middle panel) in the empirical relation (17) and the cosmological parameter  $\Omega_m$  (right panel) for 100 simulations in the fiducial case. The blue means with error bars (the chocolate means with error bars) indicate that the assumed  $\alpha = 0.9$ ,  $\beta = 65$  or  $\Omega_m = 0.3153$  (indicated by the magenta dashed lines) are consistent (inconsistent) with the mock type Ib FRBs within  $1\sigma$  region, respectively. In each panel,  $n$  and  $100 - n$  are the numbers of blue and chocolate means with error bars, respectively.  $\langle\sigma\rangle$  is the mean of the uncertainties of 100 constraints on the parameters  $\alpha$  (left panel),  $\beta$  (middle panel) and  $\Omega_m$  (right panel), respectively. See Sec. IV B for details.

construction around the world, especially the promising Square Kilometre Array (SKA) in Australia and South Africa, FAST Array (FASTA) in China, while FRB detection has been one of the main scientific goals in the ambitious visions of many countries. The era of FRBs is coming in the near future. Let us be optimistical and keep an open mind). As mentioned above, we obtain the distance modulus of type Ib FRB at low redshift by equaling it to the one of SNIa in the same host galaxy. As is well known, currently the distance modulus  $\mu$  of SNIa can be measured very precisely. It is expected that the precision will be significantly improved in the future. For example, the expected aggregate precision of SNIa detected by the Roman Space Telescope (formerly WFIRST, planned for launch in the mid-2020s) is 0.2% at  $z < 1$  [50]. So, in the fiducial case, we set the relative error  $\sigma_{\mu, \text{rel}} = 0.2\%$  for type Ib FRBs at low redshifts. Of course, we need a redshift divide  $z_d$  to define “low” ( $z < z_d$ ) and “high” ( $z \geq z_d$ ) redshifts. In the fiducial case, we set  $z_d = 0.5$ .

Following the instructions in Sec. III, we calibrate the empirical relation (17) by using type Ib FRBs at low redshifts  $z < z_d$  (note that directly fitting the empirical relation to the data at low redshifts is the way extensively used in the similar field of calibrating long GRBs as standard candles (see e.g. [24, 25])). It is expected that the correlation between  $\alpha$  and  $\beta$  would diminish significantly if the mean values of  $F_\nu$  and  $S_\nu$  are subtracted from each object, namely centering the data (we thank the referee for pointing out this issue). One might try this way alternatively, while we leave it here as an open topic). To this end, we use the Markov Chain Monte Carlo (MCMC) code Cobaya [51], which is the Python version of the well-known CosmoMC [52]. Fitting the empirical relation given by Eq. (17) to the data of type Ib FRBs at low redshifts  $z < z_d$ , we find the marginalized  $1\sigma$  constraints on the parameters  $\alpha$  and  $\beta$ , namely

$$\alpha = 0.8997^{+0.0005}_{+0.0005}, \quad \beta = 64.9282^{+0.1347}_{-0.1209}, \quad (24)$$

and we also present the contours and the marginalized probability in Fig. 1. Then, assuming the calibrated empirical relation (17) with  $\alpha$  and  $\beta$  given in Eq. (24) still holds at high redshifts  $z \geq z_d$ , we can derive the distance moduli  $\mu$  for type Ib FRBs at high redshifts  $z \geq z_d$  with their observed fluences  $F_{\nu, \text{obs}}$  and fluxes  $S_{\nu, \text{obs}}$ . Their errors  $\sigma_\mu$  can also be obtained by using the error propagation. In the left panel of Fig. 2, we present the Hubble diagram  $\mu$  versus  $z$  for type Ib FRBs at high redshifts  $z \geq z_d$ , while the error bars  $\sigma_\mu$  are also plotted. Fitting the flat  $\Lambda$ CDM cosmology given by Eq. (20) to the distance moduli  $\mu(z_i)$  data of type Ib FRBs at high redshifts  $z \geq z_d$ , we obtain the  $1\sigma$  constraint on  $\Omega_m$ , namely

$$\Omega_m = 0.3260^{+0.0362}_{-0.0475}, \quad (25)$$

while the Hubble constant  $H_0$  has been marginalized. We also present the marginalized probability in the right panel of Fig. 2. Clearly, the assumed value  $\Omega_m = 0.3153$  used in Sec. IV A to generate the mock type Ib FRBs is well consistent with the one in Eq. (25).

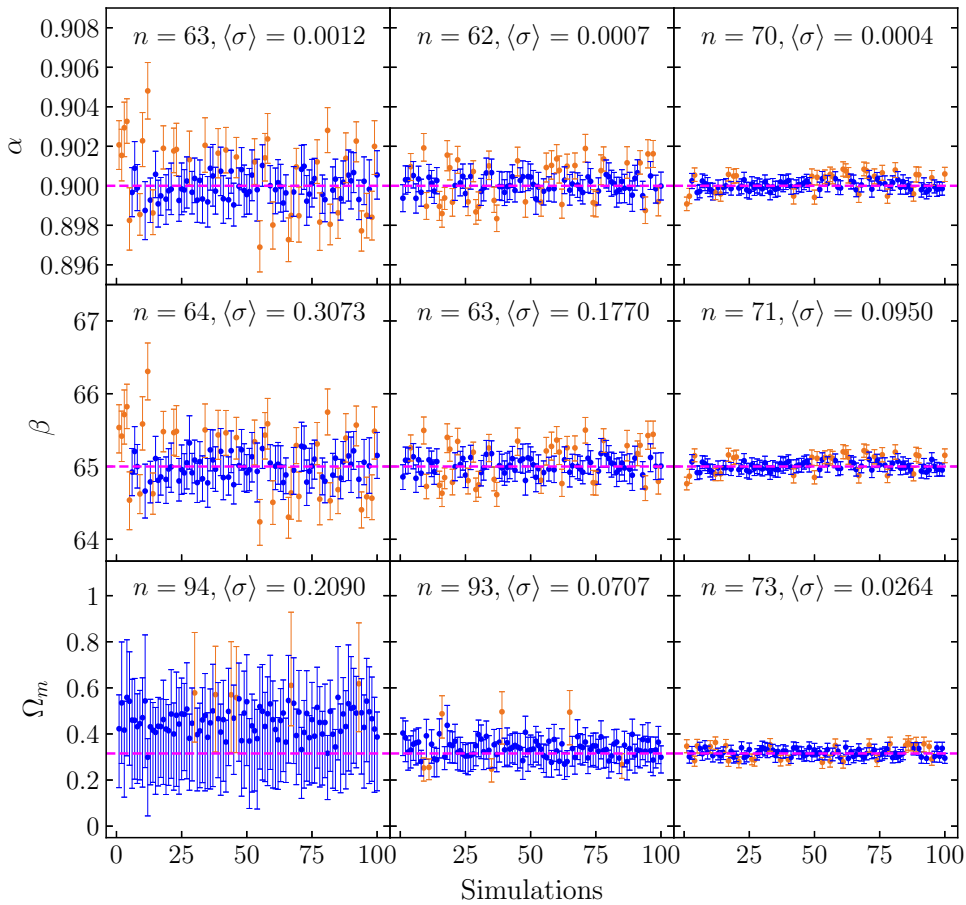


FIG. 4: The same as in Fig. 3, but for the cases of  $N_{\text{FRB}} = 100$  (left panels), 300 (middle panels) and 1000 (right panels) type Ib FRBs, respectively. Fig. 3 ( $N_{\text{FRB}} = 500$ ) should be viewed together. See Sec. IV C for details.

To avoid the statistical noise due to random fluctuations, one should repeat the above constraints for a large number of simulations. But it is expensive to consider too many simulations since they consume a large amount of computation power and time. As a balance, here we consider 100 simulations, which is enough actually (in principle, the number is “large enough” to repeat at least  $\mathcal{O}(10^6)$  simulations, but it is too expensive for us. On the other hand, there is no significant difference between  $\mathcal{O}(10^2)$  and  $\mathcal{O}(10^3)$  simulations. One might try  $\mathcal{O}(10^4)$  simulations to this end, but we have to only consider the affordable 100 simulations in the present work to save our poor computational resource). In Fig. 3, we present the marginalized  $1\sigma$  constraints on the parameters  $\alpha$ ,  $\beta$  in the empirical relation (17) and the cosmological parameter  $\Omega_m$  for 100 simulations in the fiducial case. It is easy to see from Fig. 3 that the assumed values  $\alpha = 0.9$ ,  $\beta = 65$ , and  $\Omega_m = 0.3153$  used in Sec. IV A to generate the mock type Ib FRBs can be found within  $1\sigma$  region in most of the 100 simulations ( $\sim 70\%$  for  $\alpha$  and  $\beta$ ,  $86\%$  for  $\Omega_m$ ). This implies that the constraints from these mock type Ib FRBs are fairly reliable and robust. The pipeline of calibrating type Ib FRBs as standard candles to study cosmology works well. In the followings, we will test the key factors affecting the calibration and the cosmological constraints, by considering other cases different from the fiducial case.

### C. The number of type Ib FRBs

In the fiducial case, we have set  $N_{\text{FRB}} = 500$ ,  $z_d = 0.5$ ,  $\sigma_{\mu, \text{rel}} = 0.2\%$ , and  $\sigma_{F, \text{rel}} = \sigma_{S, \text{rel}} = 1\%$ . Clearly, the number of type Ib FRBs (namely  $N_{\text{FRB}}$ ) plays an important role. It is easy to expect that the constraints become better for the larger  $N_{\text{FRB}}$ . However, the time we have to wait becomes longer to accumulate a larger amount of type Ib FRBs with identified redshifts. So, the suitable question is how many type Ib FRBs with identified redshifts are enough to get the acceptable constraints?

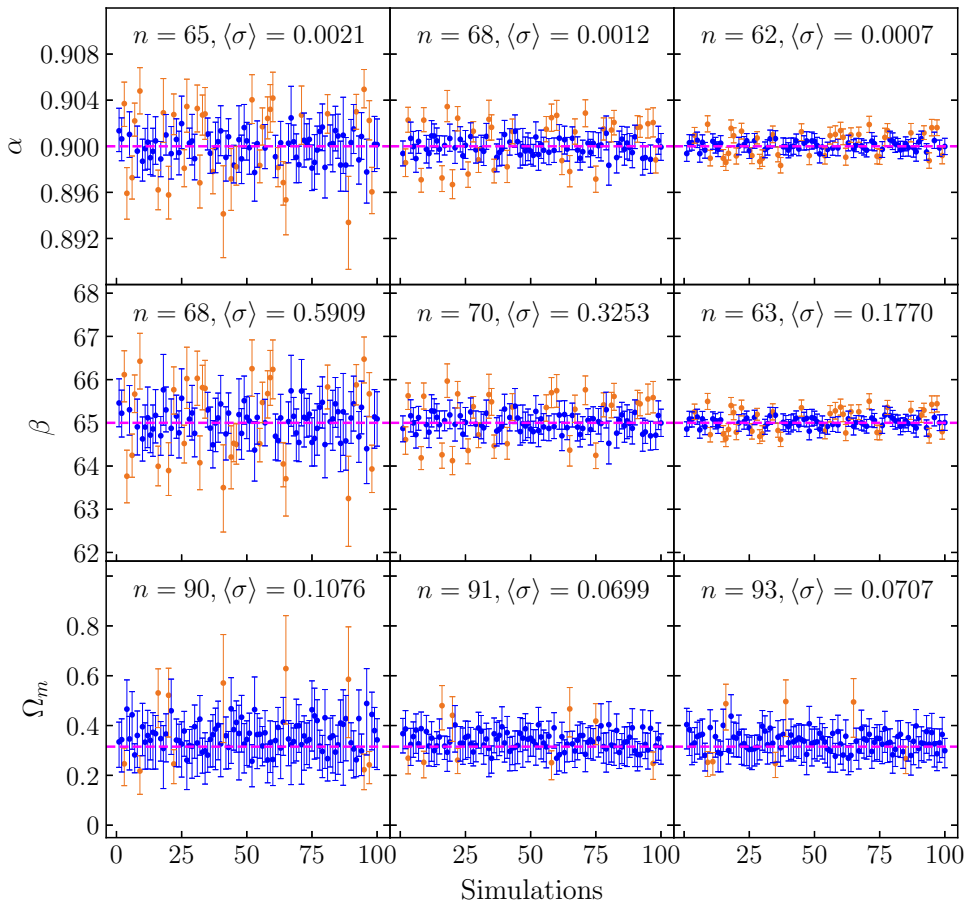


FIG. 5: The same as in Fig. 3, but for the cases of  $N_{\text{FRB}} = 300$  and  $z_d = 0.1$  (left panels), 0.2 (middle panels) and 0.5 (right panels), respectively. See Sec. IV D for details.

Here, we modify the fiducial case by considering  $N_{\text{FRB}} = 100, 300$ , and 1000, while the other settings keep unchanged. Following the similar pipeline in Sec. IV B for the fiducial case, in Fig. 4 we present the marginalized  $1\sigma$  constraints on the parameters  $\alpha, \beta$  in the empirical relation (17) and the cosmological parameter  $\Omega_m$  for 100 simulations in the cases of  $N_{\text{FRB}} = 100, 300$ , and 1000. Note that Fig. 4 should be viewed together with Fig. 3 ( $N_{\text{FRB}} = 500$ ). It is easy to see from Figs. 3 and 4 that the assumed values  $\alpha = 0.9, \beta = 65$ , and  $\Omega_m = 0.3153$  used in Sec. IV A to generate the mock type Ib FRBs can be found within  $1\sigma$  region in most of the 100 simulations (namely  $62 \sim 71\%$  for  $\alpha$  and  $\beta$ ,  $73 \sim 94\%$  for  $\Omega_m$ ). This implies that the constraints from these mock type Ib FRBs are fairly reliable and robust. Clearly, we find from Figs. 3 and 4 that the constraints on  $\alpha, \beta$  and  $\Omega_m$  become better for larger  $N_{\text{FRB}}$ , as expected. In particular, the mean of the uncertainties  $\langle \sigma \rangle = 0.2090$  for  $\Omega_m$  in the case of  $N_{\text{FRB}} = 100$  (bottom-left panel of Fig. 4) is too large ( $\sim 66\%$ ) compared with the assumed value  $\Omega_m = 0.3153$ . So,  $N_{\text{FRB}} = 100$  is not enough to get the acceptable constraints. But the cases of  $N_{\text{FRB}} = 300$  and 500 are acceptable, since the uncertainties decrease dramatically. Although  $N_{\text{FRB}} = 1000$  is best, the cost is expensive to accumulate such a large amount of type Ib FRBs with identified redshifts (note that as mentioned in Sec. III (namely in the next paragraph below Eq. (18)), we estimate that  $N_{\text{FRB}}$  could be  $\sim \mathcal{O}(10^3)$  in the next 10 years with the future giant telescopes/arrays such as SKA and FASTA). So, we only consider the cases of  $N_{\text{FRB}} = 300$  and 500 in the followings.

#### D. The redshift divide

It is expected that the closer FRBs are easier to be detected and localized in the host galaxies. So, the lower redshift divide  $z_d$  might be better. But it cannot be very low, otherwise there will be not enough

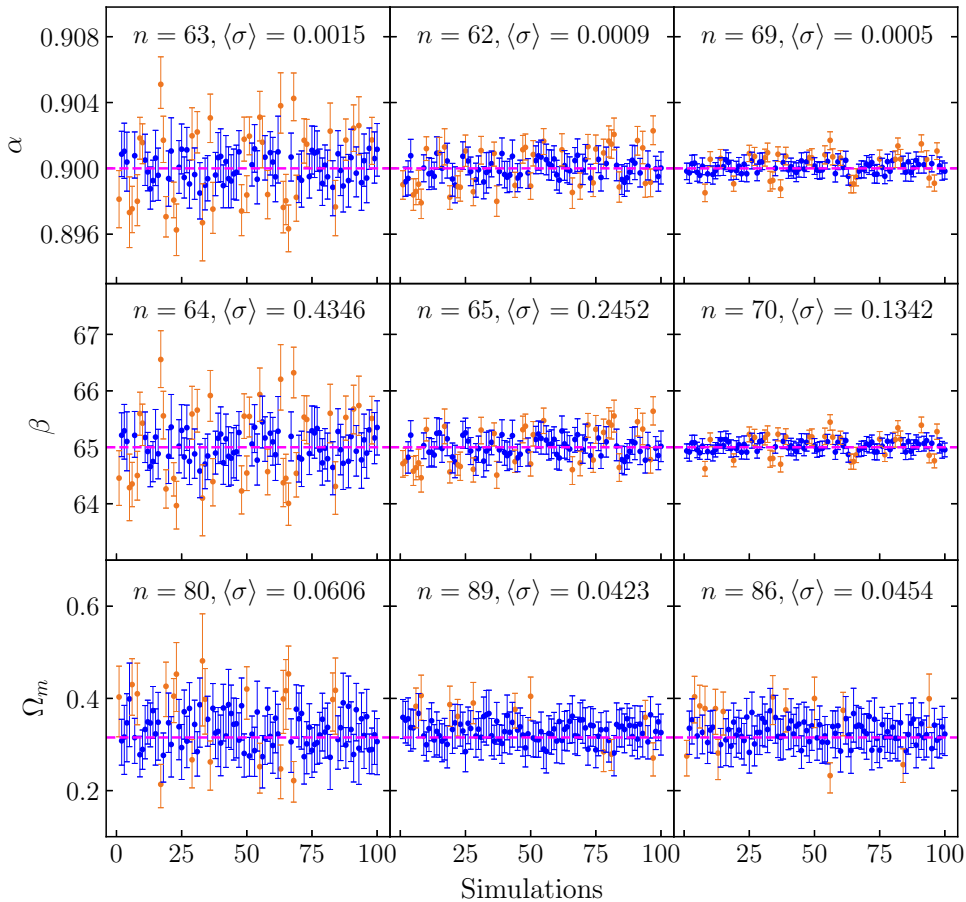


FIG. 6: The same as in Fig. 3, but for the cases of  $N_{\text{FRB}} = 500$  and  $z_d = 0.1$  (left panels), 0.2 (middle panels) and 0.5 (right panels), respectively. See Sec. IV D for details.

type Ib FRBs at  $z < z_d$  to calibrate the empirical relation (17) with an acceptable precision. We try to find a suitable redshift divide  $z_d$  in the balance.

We consider the redshift divides  $z_d = 0.1, 0.2$  and  $0.5$  for the cases of  $N_{\text{FRB}} = 300$  and  $500$ , respectively, while the other settings of the fiducial case keep unchanged. Following the similar pipeline in Sec. IV B for the fiducial case, in Figs. 5 and 6 we present the marginalized  $1\sigma$  constraints on the parameters  $\alpha$ ,  $\beta$  and  $\Omega_m$  for 100 simulations in the cases of  $N_{\text{FRB}} = 300$  and  $500$ , respectively. We find from Figs. 5 and 6 that the constraints from the mock type Ib FRBs are fairly reliable and robust, since the assumed values  $\alpha = 0.9$ ,  $\beta = 65$ , and  $\Omega_m = 0.3153$  used in Sec. IV A to generate the mock type Ib FRBs can be found within  $1\sigma$  region in most of the 100 simulations (namely  $62 \sim 70\%$  for  $\alpha$  and  $\beta$ ,  $80 \sim 93\%$  for  $\Omega_m$ ). From Figs. 5 and 6, it is easy to see that the uncertainties  $\langle\sigma\rangle$  for  $\alpha$ ,  $\beta$  and  $\Omega_m$  in the cases of  $z_d = 0.1$  are all much larger than (about 2 times of) the ones in the cases of  $z_d = 0.2$  and  $0.5$ . Thus,  $z_d = 0.1$  is not suitable. Although the constraints on  $\alpha$  and  $\beta$  in the cases of  $z_d = 0.5$  are better than the ones in the cases of  $z_d = 0.2$ , the constraints on the cosmological parameter  $\Omega_m$  are at the same level in both cases of  $z_d = 0.5$  and  $0.2$ . In this sense, we prefer  $z_d = 0.2$  over  $0.5$  since a lower redshift divide is easier to achieve, as mentioned above. The number of type Ib FRBs ( $N_{\text{FRB}} = 300$  or  $500$ ) makes almost no difference at this point. So, we consider that  $z_d = 0.2$  might be a suitable choice on balance.

### E. The precision of the distance modulus

In the fiducial case, we have assumed that the distance modulus  $\mu$  can be measured with high precision, namely the relative error  $\sigma_{\mu, \text{rel}} = 0.2\%$  [50] in the era of the Roman Space Telescope (formerly WFIRST).

But before the launch of the Roman Space Telescope, how does this precision affect the calibration and the cosmological constraints?

We consider the relative error  $\sigma_{\mu, \text{rel}} = 0.2\%$ ,  $0.5\%$  and  $1\%$  for the cases of  $N_{\text{FRB}} = 300$  and  $500$ , respectively, while  $z_d = 0.2$  and  $\sigma_{F, \text{rel}} = \sigma_{S, \text{rel}} = 1\%$  (as in the fiducial case). Again, in Figs. 7 and 8 we present the marginalized  $1\sigma$  constraints on the parameters  $\alpha$ ,  $\beta$  and  $\Omega_m$  for 100 simulations in the cases of  $N_{\text{FRB}} = 300$  and  $500$ , respectively. We find from Figs. 7 and 8 that the constraints from the mock type Ib FRBs are fairly reliable and robust, since the assumed values  $\alpha = 0.9$ ,  $\beta = 65$ , and  $\Omega_m = 0.3153$  used in Sec. IV A to generate the mock type Ib FRBs can be found within  $1\sigma$  region in most of the 100 simulations (namely  $62 \sim 77\%$  for  $\alpha$  and  $\beta$ ,  $87 \sim 97\%$  for  $\Omega_m$ ). From Figs. 7 and 8, it is easy to see that the constraints on  $\alpha$ ,  $\beta$  and  $\Omega_m$  become worse for larger  $\sigma_{\mu, \text{rel}}$ . The number of type Ib FRBs ( $N_{\text{FRB}} = 300$  or  $500$ ) makes almost no difference at this point. In particular, the mean of the uncertainties  $\langle\sigma\rangle = 0.1724$  for  $\Omega_m$  in the case of  $N_{\text{FRB}} = 300$  and  $\sigma_{\mu, \text{rel}} = 1\%$  (bottom-right panel of Fig. 7) is too large ( $\sim 55\%$ ) compared with the assumed value  $\Omega_m = 0.3153$ . But it can decrease to  $\langle\sigma\rangle = 0.1016$  at the price of increasing the number of type Ib FRBs to  $N_{\text{FRB}} = 500$  (bottom-right panel of Fig. 8). The case of  $\sigma_{\mu, \text{rel}} = 0.2\%$  is best, while the case of  $\sigma_{\mu, \text{rel}} = 0.5\%$  is also acceptable, regardless of  $N_{\text{FRB}} = 300$  or  $500$ . Note that currently SNIa can be measured with the precision around  $0.6\%$  (see e.g. Union2.1 [53], Pantheon [54] and Pantheon+ [55, 56] SNIa samples). Thus, it is reasonable to expect  $\sigma_{\mu, \text{rel}} \leq 0.5\%$  in the near future for type Ib FRBs which share the same host galaxies with SNIa. On the other hand, if the Roman Space Telescope (formerly WFIRST) could be launched in mid-2020s as planned,  $\sigma_{\mu, \text{rel}} = 0.2\%$  [50] will be easily achieved very soon.

### F. The precisions of the fluence and the flux

In the fiducial case, we have assumed that the fluence  $F_\nu$  and the flux  $S_\nu$  could be measured with high precisions, namely the relative errors  $\sigma_{F, \text{rel}} = \sigma_{S, \text{rel}} = 1\%$ . Of course, such high precisions cannot be achieved currently in the actual data of FRBs. Since FRBs have become a very promising and thriving field in astronomy and cosmology recently, many observational efforts have been dedicated to FRBs, and hence it is reasonable to expect some breakthroughs in the observations and the instruments in the future. Thus, it is of interest to see the effects of these precisions on the calibration of type Ib FRBs and their cosmological constraints.

We consider the relative errors  $\sigma_{F, \text{rel}} = \sigma_{S, \text{rel}} = 1\%$ ,  $2\%$  and  $3\%$  for the cases of  $N_{\text{FRB}} = 300$  and  $500$ , respectively, while  $z_d = 0.2$  and  $\sigma_{\mu, \text{rel}} = 0.2\%$  (as in the fiducial case). Similarly, we present the results in Figs. 9 and 10. We find from Figs. 9 and 10 that the constraints from the mock type Ib FRBs are fairly reliable and robust, since the assumed values  $\alpha = 0.9$ ,  $\beta = 65$ , and  $\Omega_m = 0.3153$  used in Sec. IV A to generate the mock type Ib FRBs can be found within  $1\sigma$  region in most of the 100 simulations (namely  $62 \sim 74\%$  for  $\alpha$  and  $\beta$ ,  $79 \sim 91\%$  for  $\Omega_m$ ). From Figs. 9 and 10, it is easy to see that the constraints on  $\alpha$ ,  $\beta$  and  $\Omega_m$  become worse for larger  $\sigma_{F, \text{rel}} = \sigma_{S, \text{rel}}$ . The number of type Ib FRBs ( $N_{\text{FRB}} = 300$  or  $500$ ) makes almost no difference at this point. In particular, the mean of the uncertainties  $\langle\sigma\rangle = 0.2089$  for  $\Omega_m$  in the case of  $N_{\text{FRB}} = 300$  and  $\sigma_{F, \text{rel}} = \sigma_{S, \text{rel}} = 3\%$  (bottom-right panel of Fig. 9) is too large ( $\sim 66\%$ ) compared with the assumed value  $\Omega_m = 0.3153$ . Although it can decrease to  $\langle\sigma\rangle = 0.1396$  at the price of increasing the number of type Ib FRBs to  $N_{\text{FRB}} = 500$  (bottom-right panel of Fig. 10), this is still unacceptable since  $0.1396/0.3153 \simeq 44\%$ . In this sense, the case of  $\sigma_{F, \text{rel}} = \sigma_{S, \text{rel}} = 3\%$  is not enough to get the acceptable constraints on the cosmological models. One of the ways out is to significantly increase the number of type Ib FRBs (say,  $N_{\text{FRB}} = 1000$  or even more). On the other hand, the cases of  $\sigma_{F, \text{rel}} = \sigma_{S, \text{rel}} = 1\%$  and  $2\%$  are acceptable. Anyway, improving the precisions of the fluences and the fluxes for FRBs is an important task in the future.

### G. Three-parameter empirical relation

In the above discussions, the empirical relation given in Eq. (17) is considered. This is a two-parameter empirical relation, with  $\alpha$  and  $\beta$  as the free parameters. The coefficients for the terms of  $\log F_\nu$  and  $\log S_\nu$  are not independent. The cause roots in the empirical  $L_\nu - E$  relation given in Eq. (16) due to the unknown physical mechanism for the origins of type Ib FRBs.

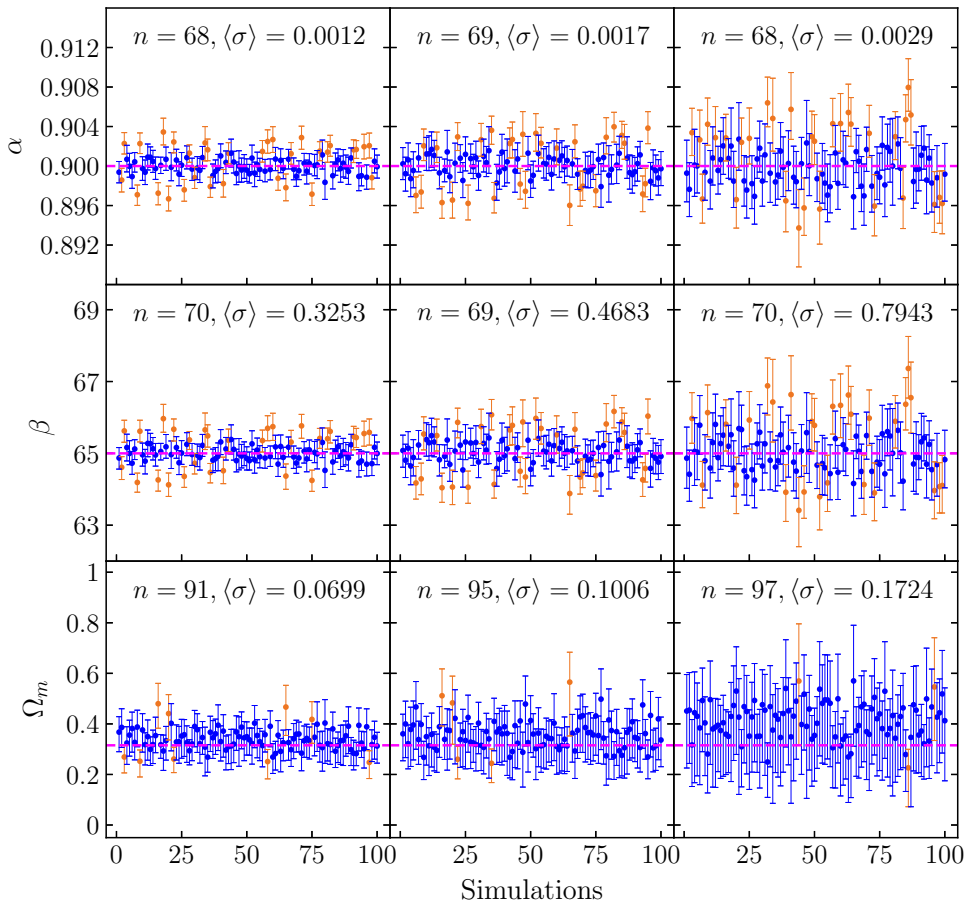


FIG. 7: The same as in Fig. 3, but for the cases of  $N_{\text{FRB}} = 300$ ,  $z_d = 0.2$ , and  $\sigma_{\mu, \text{rel}} = 0.2\%$  (left panels),  $0.5\%$  (middle panels),  $1\%$  (right panels), respectively. See Sec. IV E for details.

However, if one pretends to do not know the empirical  $L_\nu - E$  relation given in Eq. (16), the empirical relation between the distance modulus  $\mu$  (equivalently the luminosity distance  $d_L$ ), the fluence  $F_\nu$  and the flux  $S_\nu$  could be instead regarded as a three-parameter empirical relation without any underlying physical mechanism for the origins of type Ib FRBs, namely

$$\mu = A \log \frac{F_\nu / (1+z)}{\text{Jy ms}} + B \log \frac{S_\nu}{\text{Jy}} + C, \quad (26)$$

where the independent parameters  $A$ ,  $B$  and  $C$  are all dimensionless constants. The assumed underlying empirical relation given by Eq. (23) used in Sec. IV A to generate the mock type Ib FRBs corresponds to  $A = -25$ ,  $B = 22.5$  and  $C = 65$ . One can calibrate the three-parameter empirical relation (26) by using type Ib FRBs at low redshifts  $z < z_d$ , and then obtain the distance moduli  $\mu$  for type Ib FRBs at high redshifts  $z \geq z_d$  by using this calibrated three-parameter empirical relation. Thus, one can constrain the cosmological models with these type Ib FRBs at high redshifts  $z \geq z_d$ .

We consider the cases of  $N_{\text{FRB}} = 100, 300$  and  $500$  with  $z_d = 0.2$ ,  $\sigma_{\mu, \text{rel}} = 0.2\%$ , and  $\sigma_{F, \text{rel}} = \sigma_{S, \text{rel}} = 1\%$  (as in the fiducial case). In Fig. 11, we present the marginalized  $1\sigma$  constraints on the parameters  $A$ ,  $B$ ,  $C$  and  $\Omega_m$  for 100 simulations in the cases of  $N_{\text{FRB}} = 100, 300$  and  $500$ , respectively. We find from Fig. 11 that the constraints from the mock type Ib FRBs are fairly reliable and robust, since the assumed values  $A = -25$ ,  $B = 22.5$ ,  $C = 65$ , and  $\Omega_m = 0.3153$  used in Sec. IV A to generate the mock type Ib FRBs can be found within  $1\sigma$  region in most of the 100 simulations (namely  $60 \sim 69\%$  for  $A$ ,  $B$  and  $C$ ,  $67 \sim 87\%$  for  $\Omega_m$ ). Comparing Fig. 11 with the cases of two-parameter empirical relation, the uncertainties ( $\sigma$ ) become larger. This is not surprising, since the number of independent parameters has been increased. On the other hand, the mean of the uncertainties  $\langle\sigma\rangle = 0.2562$  for  $\Omega_m$  in the case of  $N_{\text{FRB}} = 100$  (bottom-left panel of Fig. 11) is too large ( $\sim 81\%$ ) compared with the assumed value

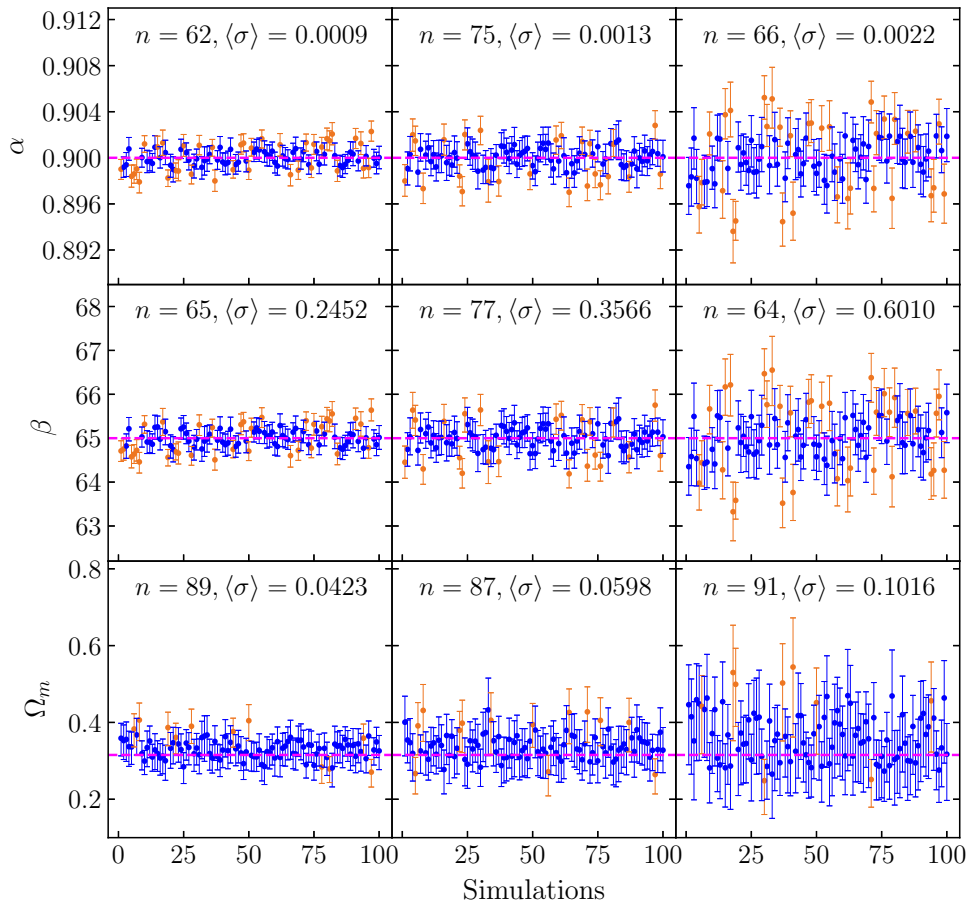


FIG. 8: The same as in Fig. 3, but for the cases of  $N_{\text{FRB}} = 500$ ,  $z_d = 0.2$ , and  $\sigma_{\mu, \text{rel}} = 0.2\%$  (left panels),  $0.5\%$  (middle panels),  $1\%$  (right panels), respectively. See Sec. IV E for details.

$\Omega_m = 0.3153$ . Thus,  $N_{\text{FRB}} = 100$  is not enough to get the acceptable constraints. But the uncertainties dramatically decrease in the cases of  $N_{\text{FRB}} = 300$  and  $500$ , and hence they are acceptable. Comparing with the middle panels of Fig. 5 ( $N_{\text{FRB}} = 300$ ) and Fig. 6 ( $N_{\text{FRB}} = 500$ ) in the case of two-parameter empirical relation, we find that the constraints on the cosmological parameter  $\Omega_m$  become looser in the case of three-parameter empirical relation. So, we consider that the two-parameter empirical relation (17) should be preferred in the FRB cosmology.

## V. CONCLUDING REMARKS

Recently, FRBs have become a thriving field in astronomy and cosmology. Due to their extragalactic and cosmological origin, they are useful to study the cosmic expansion and IGM. In the literature, the dispersion measure DM of FRB has been considered extensively. It could be used as an indirect proxy of the luminosity distance  $d_L$  of FRB. The observed DM contains the contributions from the Milky Way (MW), the MW halo, IGM, and the host galaxy. Unfortunately, IGM and the host galaxy of FRB are poorly known to date, and hence the large uncertainties of  $\text{DM}_{\text{IGM}}$  and  $\text{DM}_{\text{host}}$  in DM plague the FRB cosmology. Could we avoid DM in studying cosmology? Could we instead consider the luminosity distance  $d_L$  directly in the FRB cosmology? We are interested to find a way out for this problem in the present work. From the lessons of calibrating SNIa or long GRBs as standard candles, we consider a universal subclassification scheme for FRBs, and there are some empirical relations for them. In the present work, we propose to calibrate type Ib FRBs as standard candles by using a tight empirical relation without DM. The calibrated type Ib FRBs at high redshifts can be used like SNIa to constrain the cosmological models. We also test the key factors affecting the calibration and the cosmological constraints.



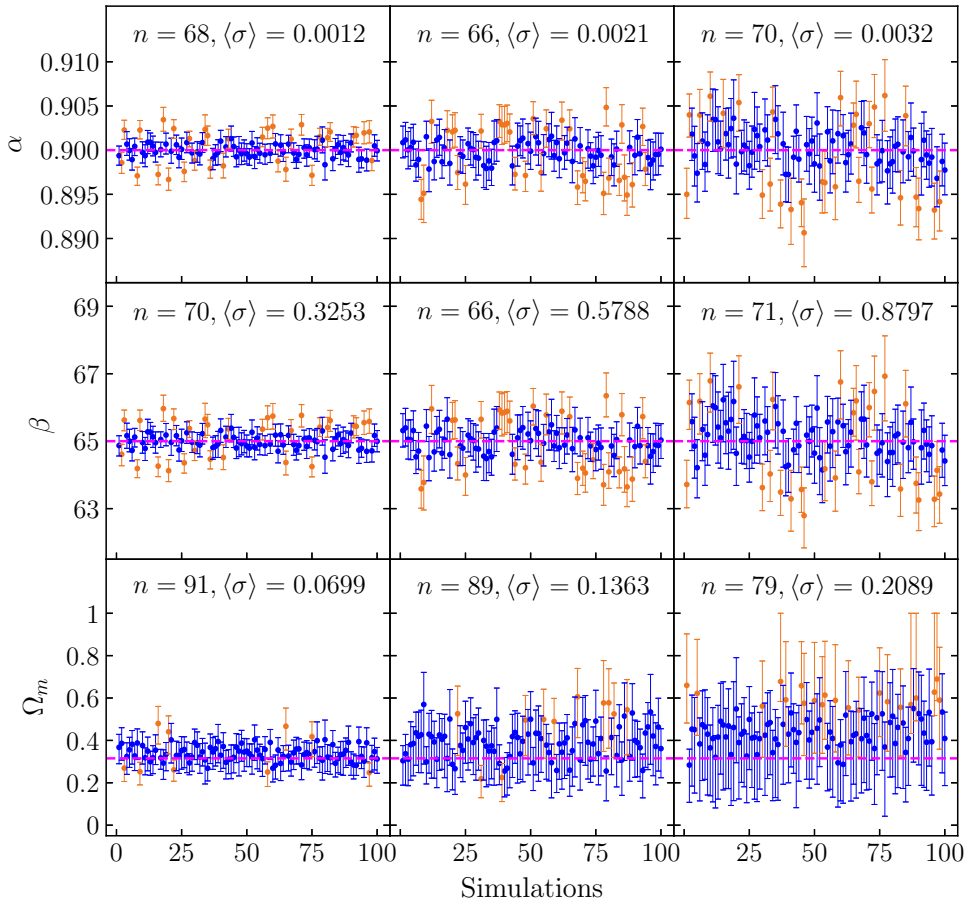


FIG. 9: The same as in Fig. 3, but for the cases of  $N_{\text{FRB}} = 300$ ,  $z_d = 0.2$ ,  $\sigma_{\mu, \text{rel}} = 0.2\%$ , and  $\sigma_{F, \text{rel}} = \sigma_{S, \text{rel}} = 1\%$  (left panels),  $2\%$  (middle panels),  $3\%$  (right panels), respectively. See Sec. IV F for details.

We find that the constraints become better for the larger number of type Ib FRBs.  $N_{\text{FRB}} = 100$  is not enough to get the acceptable constraints, while  $N_{\text{FRB}} = 300$  or  $500$  are suitable. We also find that the redshift divide  $z_d = 0.1$  is not suitable, and we suggest that  $z_d = 0.2$  might be a suitable choice on balance. It is found that the precision of the distance modulus  $\sigma_{\mu, \text{rel}} \leq 0.5\%$  is enough to get the acceptable constraints, which can be achieved very soon. On the other hand, the precisions of the fluence and the flux  $\sigma_{F, \text{rel}} = \sigma_{S, \text{rel}} \geq 3\%$  is not enough to get the acceptable constraints on the cosmological models. One of the ways out is to significantly increase the number of type Ib FRBs (say,  $N_{\text{FRB}} = 1000$  or even more). Anyway, improving the precisions of the fluences and the fluxes for FRBs is an important task in the future. Although one could instead consider a three-parameter empirical relation (26), we suggest that the two-parameter empirical relation (17) should be preferred in the FRB cosmology.

Of course, current data of FRBs are certainly not enough to calibrate type Ib FRBs as standard candles. So, it is a proof of concept by using the simulated FRBs in the present work. But the same pipeline holds for the actual type Ib FRBs in the future. Since FRBs have become a very promising and thriving field in astronomy and cosmology recently, many observational efforts have been dedicated to FRBs, and hence it is reasonable to expect some breakthroughs in the observations and the instruments in the future. Let us be optimistic with the hope to actually use type Ib FRBs as standard candles.

Clearly, the key to calibrate type Ib FRBs as standard candles is that there is really a tight empirical relation for them, due to the unknown physical mechanism for the origins of type Ib FRBs. The universal subclassification scheme for FRBs proposed in [16] and the empirical relations found in [16] should be carefully examined by using the larger and better FRB datasets in the future. On the other hand, the theories that could produce such an empirical relation for type Ib FRBs are desirable.

Notice that in the present work we constrain the cosmological model by using the calibrated type Ib FRBs at high redshifts alone. But this is not necessary. In fact, similar to the case of SNIa, it is better

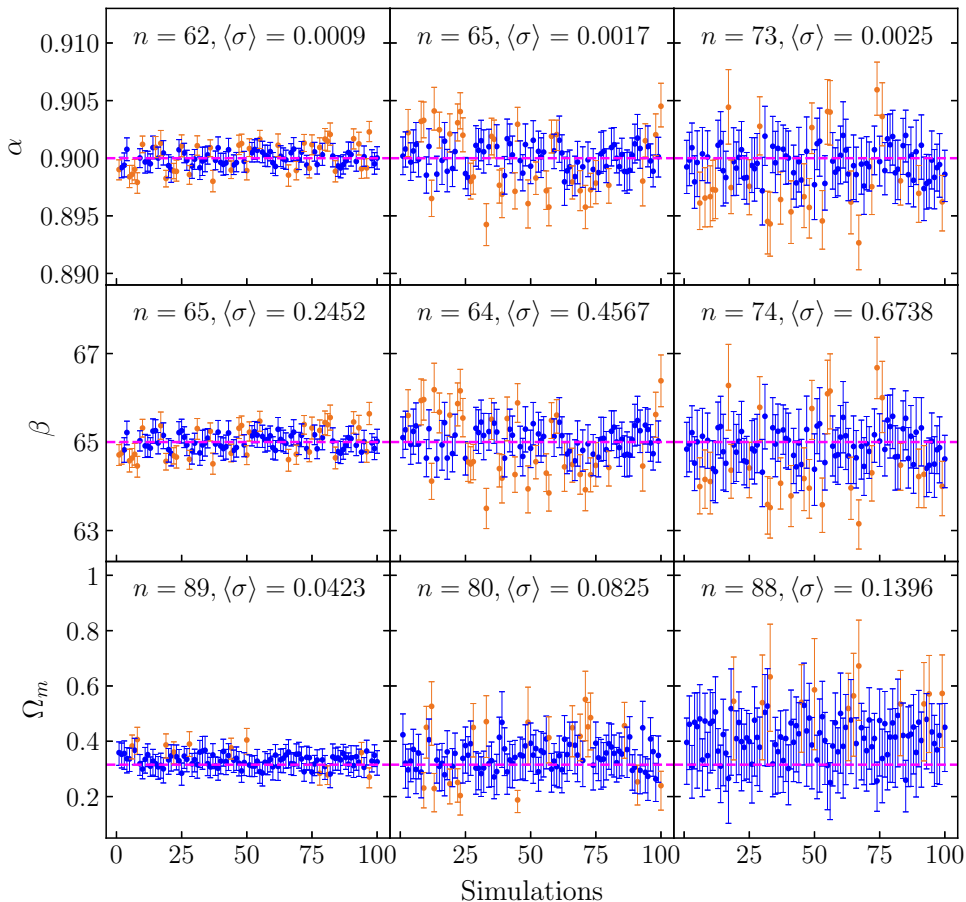


FIG. 10: The same as in Fig. 3, but for the cases of  $N_{\text{FRB}} = 500$ ,  $z_d = 0.2$ ,  $\sigma_{\mu, \text{rel}} = 0.2\%$ , and  $\sigma_{F, \text{rel}} = \sigma_{S, \text{rel}} = 1\%$  (left panels), 2% (middle panels), 3% (right panels), respectively. See Sec. IV F for details.

to combine them with other observations (e.g. cosmic microwave background (CMB) and large-scale structure (LSS)) to obtain the much tighter cosmological constraints.

In the present work, the subclasses of FRBs are called type I, II, a, b, Ia, Ib, IIa, IIb FRBs as in [16], respectively. However, these terms might be hard to remember. So, the alternative terms nFRBs, rFRBs, oFRBs, yFRBs, noFRBs, nyFRBs, roFRBs, ryFRBs are suggested in [61], which might be friendly and easy to remember. We refer to [61] for more details.

Several years passed after the first CHIME/FRB catalog [42]. To date, more than 50 FRBs have been well localized, and hence their redshifts  $z$  are observationally known. In [61], the empirical relations have been carefully checked with the actual data of current localized FRBs. It has been found in [61] that many empirical relations for FRBs still hold. In particular, the empirical  $L_\nu - E$  relation used here to calibrate FRBs as standard candles for cosmology stands firm with the current 44  $\sim$  52 localized FRBs, and its slope  $a$  and intercept  $b$  obtained from the actual data are fairly close to the ones in Eq. (9). Note that the uncertainties are also taken into account in [61]. It is found that the slope  $a \neq 1$  in the empirical  $L_\nu - E$  relation (16) far beyond  $3\sigma$  confidence level (C.L.), actually on the edge of  $4\sigma$  C.L. [61]. If  $a = 1$ , the luminosity distance  $d_L$  will be canceled in both sides of Eq. (16) (n.b. Eq. (8)), and then it cannot be used to study cosmology. But actually  $a \neq 1$  as shown in [61] by using the current localized FRBs, and hence it supports the empirical  $L_\nu - E$  relation (16) used here to calibrate FRBs as standard candles for cosmology. We strongly refer to [61] for more details.

#### ACKNOWLEDGEMENTS

We thank the anonymous referee for quite useful comments and suggestions, which helped us to improve

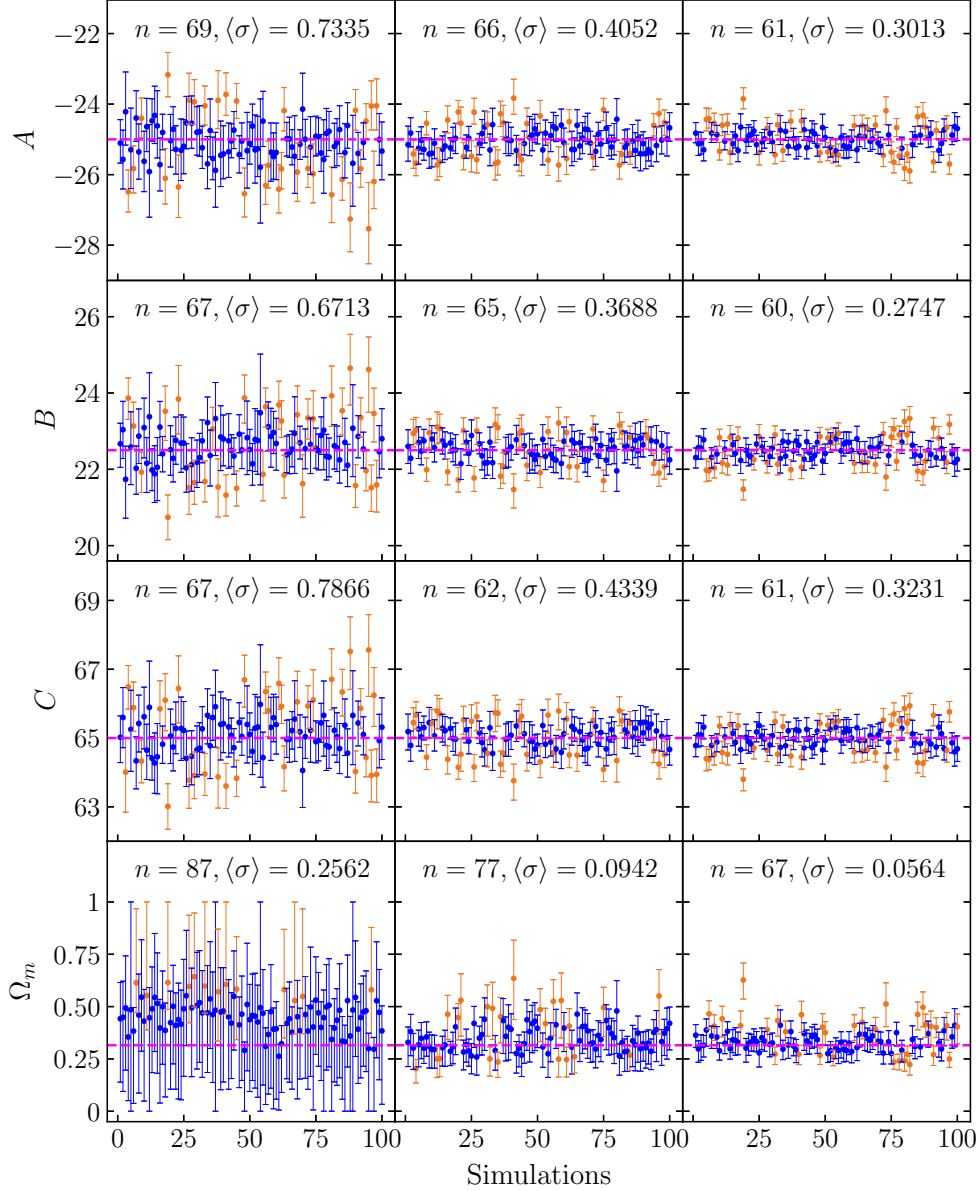


FIG. 11: The same as in Fig. 3, but for the case of three-parameter empirical relation with  $N_{\text{FRB}} = 100$  (left panels), 300 (middle panels), 500 (right panels), and  $z_d = 0.2$ ,  $\sigma_{\mu, \text{rel}} = 0.2\%$ ,  $\sigma_{F, \text{rel}} = \sigma_{S, \text{rel}} = 1\%$ . See Sec. IV G for details.

this work. We are grateful to Da-Chun Qiang, Hua-Kai Deng, Shupeng Song, Jing-Yi Jia, Shu-Ling Li, Yun-Long Wang, Lin-Yu Li and Jia-Lei Niu for kind help and useful discussions. This work was supported in part by NSFC under Grants No. 12375042, No. 11975046 and No. 11575022.

[1] <https://www.nature.com/collections/rswtktxcln>

[2] D. R. Lorimer, *Nat. Astron.* **2**, 860 (2018) [arXiv:1811.00195].

[3] E. F. Keane, *Nat. Astron.* **2**, 865 (2018) [arXiv:1811.00899].

[4] E. Petroff, J. W. T. Hessels and D. R. Lorimer, *Astron. Astrophys. Rev.* **30**, 2 (2022) [arXiv:2107.10113].

[5] B. Zhang, *Rev. Mod. Phys.* **95**, no.3, 035005 (2023) [arXiv:2212.03972].

- [6] B. Zhang, *Nature* **587**, 45 (2020) [arXiv:2011.03500].
- [7] D. Xiao, F. Y. Wang and Z. G. Dai, *Sci. China Phys. Mech. Astron.* **64**, 249501 (2021) [arXiv:2101.04907].
- [8] W. Deng and B. Zhang, *Astrophys. J.* **783**, L35 (2014) [arXiv:1401.0059].
- [9] Y. P. Yang and B. Zhang, *Astrophys. J.* **830**, no. 2, L31 (2016) [arXiv:1608.08154].
- [10] H. Gao, Z. Li and B. Zhang, *Astrophys. J.* **788**, 189 (2014) [arXiv:1402.2498].
- [11] B. Zhou, X. Li, T. Wang, Y. Z. Fan and D. M. Wei, *Phys. Rev. D* **89**, 107303 (2014) [arXiv:1401.2927].
- [12] D. C. Qiang, H. K. Deng and H. Wei, *Class. Quant. Grav.* **37**, 185022 (2020) [arXiv:1902.03580].
- [13] D. C. Qiang and H. Wei, *JCAP* **2004**, 023 (2020) [arXiv:2002.10189].
- [14] D. C. Qiang and H. Wei, *Phys. Rev. D* **103**, 083536 (2021) [arXiv:2102.00579].
- [15] D. C. Qiang, S. L. Li and H. Wei, *JCAP* **2201**, 040 (2022) [arXiv:2111.07476].
- [16] H. Y. Guo and H. Wei, *JCAP* **2207**, 010 (2022) [arXiv:2203.12551].
- [17] M. McQuinn, *Astrophys. J.* **780**, L33 (2014) [arXiv:1309.4451].
- [18] K. Ioka, *Astrophys. J.* **598**, L79 (2003) [astro-ph/0309200].
- [19] S. Inoue, *Mon. Not. Roy. Astron. Soc.* **348**, 999 (2004) [astro-ph/0309364].
- [20] M. Jaroszynski, *Mon. Not. Roy. Astron. Soc.* **484**, no. 2, 1637 (2019) [arXiv:1812.11936].
- [21] H. S. Leavitt and E. C. Pickering, *Harvard College Observatory Circular* **173**, 1 (1912).
- [22] M. M. Phillips, *Astrophys. J. Lett.* **413**, L105 (1993).
- [23] A. G. Riess *et al.*, *Astrophys. J. Lett.* **934**, no.1, L7 (2022) [arXiv:2112.04510].
- [24] N. Liang, W. K. Xiao, Y. Liu and S. N. Zhang, *Astrophys. J.* **685**, 354 (2008) [arXiv:0802.4262].
- [25] H. Wei, *JCAP* **1008**, 020 (2010) [arXiv:1004.4951].
- [26] L. Amati *et al.*, *Astron. Astrophys.* **390**, 81 (2002) [astro-ph/0205230].
- [27] B. E. Schaefer, *Astrophys. J.* **660**, 16 (2007) [astro-ph/0612285].
- [28] H. Wei and S. N. Zhang, *Eur. Phys. J. C* **63**, 139 (2009) [arXiv:0808.2240].
- [29] J. Liu and H. Wei, *Gen. Rel. Grav.* **47**, no.11, 141 (2015) [arXiv:1410.3960].
- [30] B. C. Andersen *et al.*, *Nature* **587**, no. 7832, 54 (2020) [arXiv:2005.10324].
- [31] C. D. Bochenek *et al.*, *Nature* **587**, no. 7832, 59 (2020) [arXiv:2005.10828].
- [32] L. Lin *et al.*, *Nature* **587**, no. 7832, 63 (2020) [arXiv:2005.11479].
- [33] C. K. Li *et al.*, *Nat. Astron.* **5**, 378 (2021) [arXiv:2005.11071].
- [34] S. P. Tendulkar *et al.*, *Astrophys. J. Lett.* **834**, no.2, L7 (2017) [arXiv:1701.01100].
- [35] B. Marcote *et al.*, *Nature* **577**, no.7789, 190 (2020) [arXiv:2001.02222].
- [36] C. H. Niu *et al.*, *Nature* **606**, no.7916, 873 (2022) [arXiv:2110.07418].
- [37] M. Bhardwaj *et al.*, *Astrophys. J. Lett.* **919**, no.2, L24 (2021) [arXiv:2108.12122].
- [38] M. Bhardwaj *et al.*, *Astrophys. J. Lett.* **910**, no.2, L18 (2021) [arXiv:2103.01295].
- [39] F. Kirsten *et al.*, *Nature* **602**, no.7898, 585 (2022) [arXiv:2105.11445].
- [40] K. Nimmo *et al.*, *Nat. Astron.* **6**, 393 (2022) [arXiv:2105.11446].
- [41] R. C. Zhang and B. Zhang, *Astrophys. J. Lett.* **924**, no.1, L14 (2022) [arXiv:2109.07558].
- [42] M. Amiri *et al.*, *Astrophys. J. Supp.* **257**, no.2, 59 (2021) [arXiv:2106.04352].  
The data for CHIME/FRB Catalog 1 in machine-readable format can be found via their public webpage at <https://www.chime-frb.ca/catalog>
- [43] R. C. Zhang *et al.*, *Mon. Not. Roy. Astron. Soc.* **501**, no.1, 157 (2021) [arXiv:2011.06151].
- [44] B. Marcote *et al.*, *PoS EVN2021*, 035 (2021) [arXiv:2202.11644].
- [45] B. Marcote and Z. Paragi, *PoS EVN2018*, 013 (2019) [arXiv:1901.08541].
- [46] B. Zhang, *Astrophys. J. Lett.* **867**, no.2, L21 (2018) [arXiv:1808.05277].
- [47] K. E. Heintz *et al.*, *Astrophys. J.* **903**, 152 (2020) [arXiv:2009.10747].  
The up-to-date compilation of all known FRB host galaxies is available at <https://frbhosts.org>
- [48] N. Aghanim *et al.*, *Astron. Astrophys.* **641**, A6 (2020) [arXiv:1807.06209].
- [49] P. Madau and T. Fragos, *Astrophys. J.* **840**, no.1, 39 (2017) [arXiv:1606.07887].
- [50] D. Spergel *et al.*, arXiv:1305.5425 [astro-ph.IM].
- [51] J. Torrado and A. Lewis, *JCAP* **2105**, 057 (2021) [arXiv:2005.05290],  
available at <https://cobaya.readthedocs.org>
- [52] A. Lewis and S. Bridle, *Phys. Rev. D* **66**, 103511 (2002) [astro-ph/0205436],  
available at <https://cosmologist.info/cosmomc/>
- [53] N. Suzuki *et al.*, *Astrophys. J.* **746**, 85 (2012) [arXiv:1105.3470].
- [54] D. M. Scolnic *et al.*, *Astrophys. J.* **859**, no.2, 101 (2018) [arXiv:1710.00845].

- [55] D. Scolnic *et al.*, *Astrophys. J.* **938**, no.2, 113 (2022) [arXiv:2112.03863].
- [56] D. Brout *et al.*, *Astrophys. J.* **938**, no.2, 110 (2022) [arXiv:2202.04077].
- [57] S. Bhandari *et al.*, *Astrophys. J.* **948**, no.1, 67 (2023) [arXiv:2211.16790].
- [58] K. Sharma *et al.*, *Astrophys. J.* **950**, no.2, 175 (2023) [arXiv:2302.14782].
- [59] D. Michilli *et al.*, *Astrophys. J.* **950**, no.2, 134 (2023) [arXiv:2212.11941].
- [60] C. J. Law *et al.*, *Astrophys. J.* **967**, no.1, 29 (2024) [arXiv:2307.03344].
- [61] L. Y. Li, J. Y. Jia, D. C. Qiang and H. Wei, arXiv:2408.12983 [astro-ph.HE].
- [62] E. Platts *et al.*, *Phys. Rept.* **821**, 1 (2019) [arXiv:1810.05836].  
The living theory catalogue for FRBs is available at <https://frbtheorycat.org>
- [63] J. Tian *et al.*, *Mon. Not. Roy. Astron. Soc.* **533**, no.3, 3174 (2024) [arXiv:2408.10988].
- [64] K. Sharma *et al.* arXiv:2409.16964 [astro-ph.HE].
- [65] L. Connor *et al.* arXiv:2409.16952 [astro-ph.CO].